EUROPEAN JOURNAL OF BIOMEDICAL AND PHARMACEUTICAL SCIENCES
http://www.ejbps.com

ISSN 2349-8870
Volume: 1
Issue: 3
157-167
Year: 2014

# SYNTHESIS, CHARACTERIZATION AND ELECTRICAL PROPERTIES OF POLY (N –N METHOXYANILINE)/MODIFIED MWCNT CONDUCTING POLYMER COMPOSITES

**Debabrata Ash[1], S.S Nayak[2], *P.L. Nayak[3]**

[1]F.M College, Balasore, India.

[2]CUTM, Bhubaneswar, India.

[3]Research Foundation, SIT, Parlakhemundi, India.

**Article Received on 01/10/2014** **Article Revised on 22/10/2014** **Article Accepted on 14/11/2014**

***Correspondence for Author**
**Dr. P.L. Nayak**
Research Foundation, SIT, Parlakhemundi, India.

## ABSTRACT

PMA/c-MWCNTs nanocomposites were prepared via in situ polymerization method. SEM and TEM measurement results show that the c-MWCNTs were homogeneously dispersed in the copolymer matrix. The interaction between c-MWCNTs and copolymer chain was confirmed by FTIR. The nanocomposites showed higher thermal stabilities in comparison with the bare copolymer was confirmed by TGA and DSC. The highly ordered structures of nanocomposites were confirmed by XRD patterns. In addition, the versatility of this method could be extended to prepare other polymer/ CNT nanocomposites by choosing appropriate experimental conditions. Room temperature conductivity of nanocomposite increased several times as increasing of percentage of c-MWCNT.

**KEYWORDS:** MWCNT, c-MWCNT, poly (N-N methoxyaniline), nanocomposites.

## 1. INTRODUCTION

Carbon nanotubes (CNTs) including multi-walled and single-walled carbon nanotubes (MWCNTs and SWCNTs, respectively) with exceptional structural, mechanical and electronic properties, have received considerable interest in fabricating advanced functional materials. [1-8] but insolubility of pristine CNTs in solvents and lack of compatibility with polymers cause bad dispersion of CNTs and block the application of such composites

Therefore, it is necessary to introduce the strength of binding between MWCNTs and conjugated polymers to increase interaction between components in the composites. The best way to solve the problem is to create functional groups on the back bone of MWCNT. Attachment of functional groups to MWCNTs can increase the solubility of nanotubes in solvents for better processing. [8-20] Modified MWCNTs can be easily fixed on the interface via chemical bonds or doping effect such as PANI nano-structures doped with sulfonated MWCNTs via a self-assembled process. However, the major disadvantage of PANI/CNT is its insolubility in common organic solvents and its infusibility. Preparation of alkyl group substituted PANI/CNT is a method to obtain soluble PANI/CNT composites. Soluble methyl-substituted PANI called poly (N-N methoxyaniline) (PMA). [20-23] have been synthesized by electrochemical and chemical method. Recently, PMT was also found to have additional advantage with respect to PANI due to its faster switching time between the oxidized and the reduced states. Figure.3.26 shows the outlines of the four different oxidation states of PMT.

In the present communication, we wish to describe the synthesis and characterization of PMA with MWCNT fabricated by in situ polymerization. The nanocomposites were characterized by a number of techniques including Fourier transform infrared spectroscopy (FTIR), scanning electron microscopy (SEM), transmission electron microscopy (TEM), X-ray diffraction (XRD), thermo gravimetry analysis (TGA), Differential scanning calorimetry (DSC) and electrical conductivity.

## 2. WORK-UP PROCEDURE

### Materials

N-N methoxyaniline was purchased from Aldrich, Multi-walled CNT (<90% purification) used in this study was purchased from Cheap Tubes (USA, 10– 20 nm diameter). Other reagents like ammonium persulfate (APS), hydrochloric, sulfuric, and nitric acid (Sigma Chemicals) were of analytical grade.

### Oxidation of MWCNT

MWCNTs were suspended in a 3:1 mixture of concentrated $H_2SO_4$ and $HNO_3$ and refluxed for 30 min in an ultrasonic bath. The solution was magnetically stirred and heated at 60 $^0$C for 24 h. This treatment provides carboxylic acid groups at defects in the surface of tubes and exfoliates graphite. The obtained c-MWCNTs were filtered through 0.2-μm polytetrafluoroethylene (PTFE) membrane filter, washed with plenty of deionized water until the pH value was around 7, and then dried at 70 $^0$C for 24 h.

**Synthesis of PMT/c-MWCNT polymer composites**

PMA/c-MWCNT composites were synthesized by in situ chemical oxidative polymerization. In a typical composite synthesis experiment, various weight ratio of c-MWCNTs were dissolved in 80mL 1M hydrochloric acid solutions and ultrasonicated over 2 h, then transferred into a 250mL beaker. 0.428 g m-toluidine monomer was added to the above c-MWCNTs suspension. Then a 20ml 1M hydrochloric acid solution containing 0.912 g ammonium persulfate (APS) was added into the suspension with constant mechanical stirring at room temperature. The reaction mixture was stirred for a further 12 h, and then filtered. The remaining filter cake was rinsed several times with distilled water and ethanol. The power thus obtained was dried under vacuum at 60 ˚C for 24 h. The % of c-MWCNT used for the composites were 0, 2, 5%.

## 3 MEASUREMENTS

**FTIR spectra**

The Fourier transform infrared (FT-IR) spectra were recorded on a Nicolet 8700 spectrometer, in the range 400–4,000 $cm^{-1}$

**SEM**

Morphology of the PMA/c-MWCNT composite was investigated using a Philip XL 30 SEM at an accelerating voltage of 25 kV. The sample was fractured at liquid nitrogen temperature and then was coated with a thin layer of gold before observation.

**TEM**

TEM experiments were performed on a Hitachi H-8100 electron microscope with an acceleration voltage of 200 kV.

**XRD**

X-ray diffraction (Rigaku, D/Max, 2,500 V, Cu-Kα radiation: 1.54056 A ° ) experiments were carried out on both the plain PMT and the composite samples. Wide-angle X-ray diffractograms were recorded at temperature of 30 $^{0}$C after isothermal crystallization at this temperature for 1 h in the range of 0–70 (2θ).

**TGA and DSC**

TGA and DSC studies were performed on a TA instrument (SDT Q600 analyzer) from 30 °C to 800 °C at a heating rate of 10 °C/min under nitrogen atmosphere.

**Conductivity**

The standard Van Der Pauw DC four-probe method was used to measure the electron transport behaviors of PMA and PMA/c-MWCNT composites. The samples of PMA and PMA/c-MWCNTs were pressed into pellet. The pellet was cut into a square. The square was placed on the four probe apparatus, providing a voltage for the corresponding electrical current could be obtained. The electrical conductivity of samples was calculated by the following formula:

**σ (S/cm) = (2.44 ×10/S) × (I/E),**

Where σ is the conductivity, S the sample side area, I the current passed through outer probes, and E the voltage drop across inner probes.

## 4. RESULTS AND DISCUSSION

**FTIR**

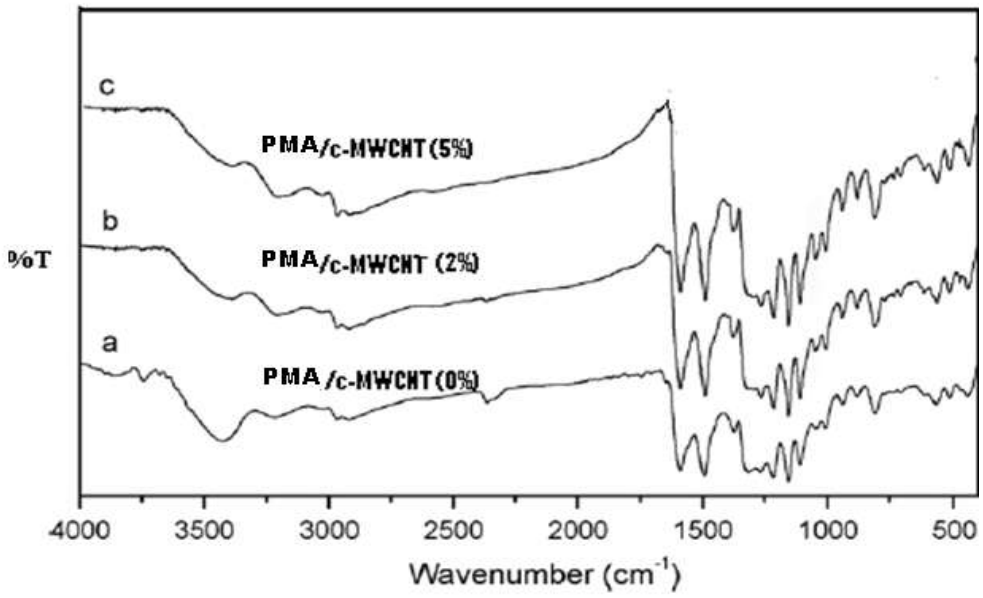


**(Figure1. FTIR of PMT/c-MWCNT)**

The FTIR spectra of PMT and PMT/c-MWCNT composites are presented in Figure.1. For PMA, the absorption band at around 3220 $cm^{-1}$ corresponds to N–H stretching mode of secondary amine. The two bands at around 1490 and 1592 $cm^{-1}$ are assigned to the stretching vibration of the benznoid and quinonoid ring. The characteristic band at 2918 $cm^{-1}$ can be assigned to the stretching vibration of the methyl ($–CH_3$) group. The band at 1375 $cm^{-1}$ is due to the symmetric deformation of methyl group. The bands at 1316 and 1210 $cm^{-1}$ can be assigned to the C–N vibration. The three bands appearing at 807, 877 and 936 $cm^{-1}$ are

attributed to an out-of-plane C–H vibration, 1, 2, 4-substitution in the benzenoid rings, and an in-plane C–H vibration of quinoid rings. All of these data are similar to the spectra of PMT salts, which confirm that the obtained sample is in its doped phase. Clearly, the FTIR spectra of PMA/c-MWCNT composites are almost identical to that of PMA, indicating that NN-methoxyaniline was polymerized on the surface of c-MWCNTs to form PMA/c-MWCNT composites.

**SEM**

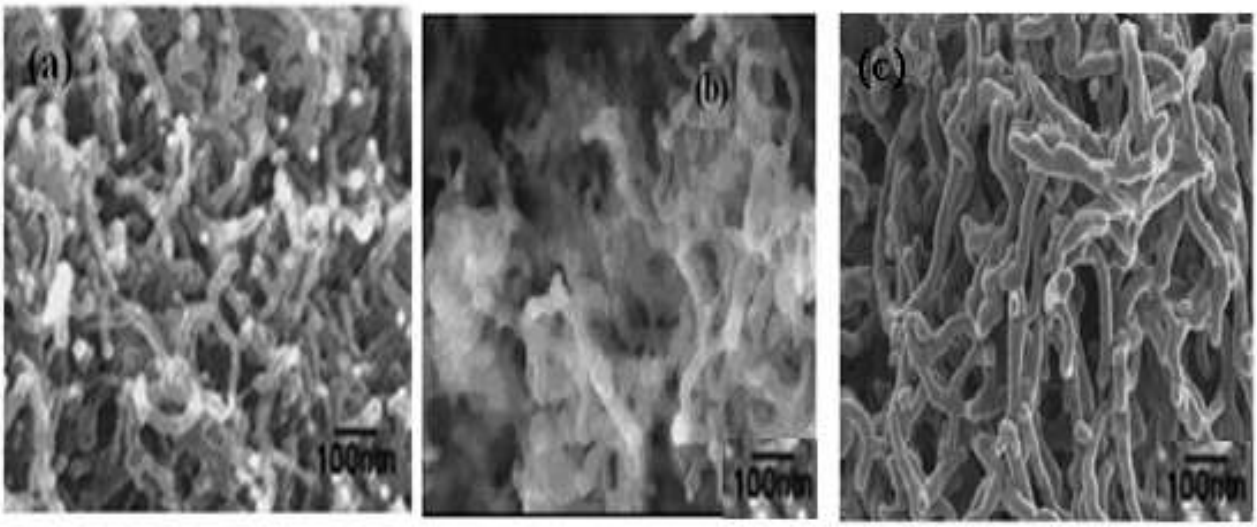


**(Figure2. SEM images of; a. c-MWCNT; b.PMT/c-MWCNT (2%); c.PMT/c-MWCNT (5%))**

The SEM pictures of the pristine c-MWCNTs, and nanocomposite with 2, and 5, % of c-MWCNTs are presented in Figure. 2(a,b,c). Figure.2a shows the disentanglement of the c-MWCNTs, and the slight reduction in the length of the nanotube is observed after oxidation with 3:1 concentrated $H_2SO_4$ and $HNO_3$ mixture. In the case of nanocomposites (Figure**.** 2b,2c), a tubular layer of coated copolymer film is clearly present on the surface of c-MWCNTs, and the diameter of the nanocomposite is increased substantially as compared to that of the c-MWCNTs, depending on the copolymer content. From these observations, it can be attributed that the coating of copolymer takes place only at the outer surface of the c-MWCNTs. The formation of the copolymer-coated tubular nanocomposite is believed to arise from the strong interaction between the co-monomer and c-MWCNTs. This interaction is thought to be made up of two components: one is the π–π electron interaction between the MWCNTs and the comonomer and the other is the hydrogen bond interaction between the carboxyl group of the c-MWCNTs and amino group of the co-monomers. Such a strong

interaction ensures that the co-monomer molecules are adsorbed on the surface of the c-MWCNTs. The polymerization of co-monomer inside the c-MWCNTs is hindered by the restricted access of the reactants to the interior of the c-MWCNTs because of the presence of the carboxyl group at the Meta position of the co-monomer. This is in agreement with the findings reported in the literature.

**TEM**

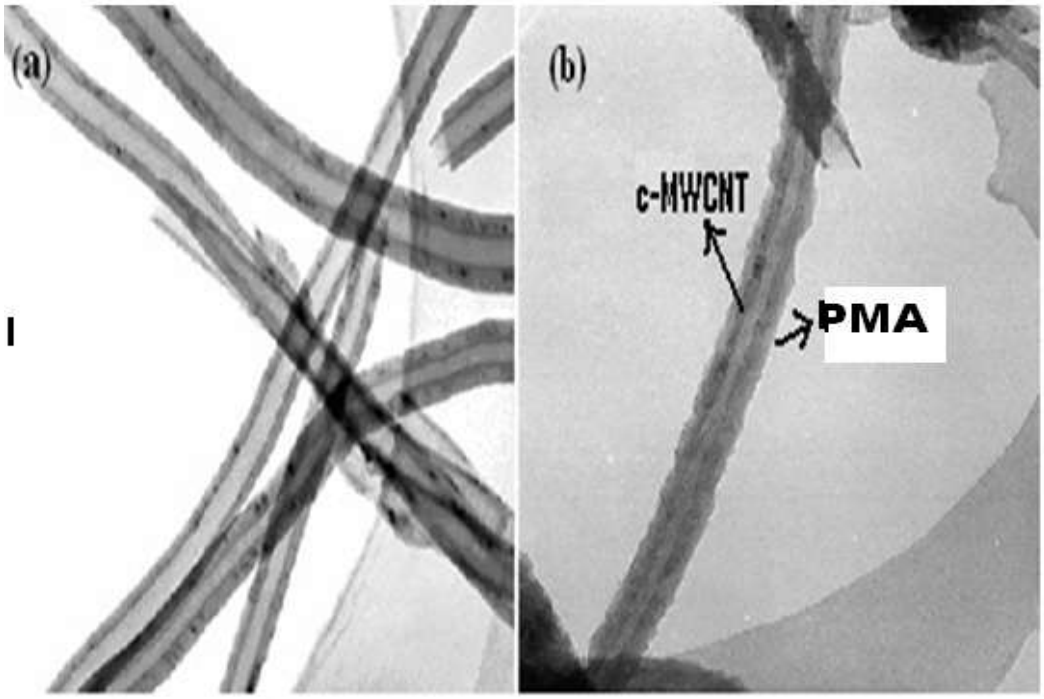


**(Figure 3: TEM image of a. MWCNT.b.PMT/c-MWCNT (5%))**

The TEM spectra of the c-MWCNT and PMA with 5% c-MWCNT are presented in Figure3.The uniform deposition of PMA on the c-MWCNT is similarly demonstrated by transmission electron microscopy (TEM), which shows the bilayered structure of coated C-MWCNT. As the internal cavity is well discernible, we conclude that the coating with PMA takes place only at the outer surface of the c-MWCNT. The polymerization of PMA inside the c-MWCNT is hindered by the restricted access of reactants to the interior of the c-MWCNT. The comonomer molecules are uniformly polymerized on the surface of c-MWCNTs and form a tubular nanocomposite. The diameter of the nanocomposite becomes larger than that of the c-MWCNTs after polymerization.

**XRD**

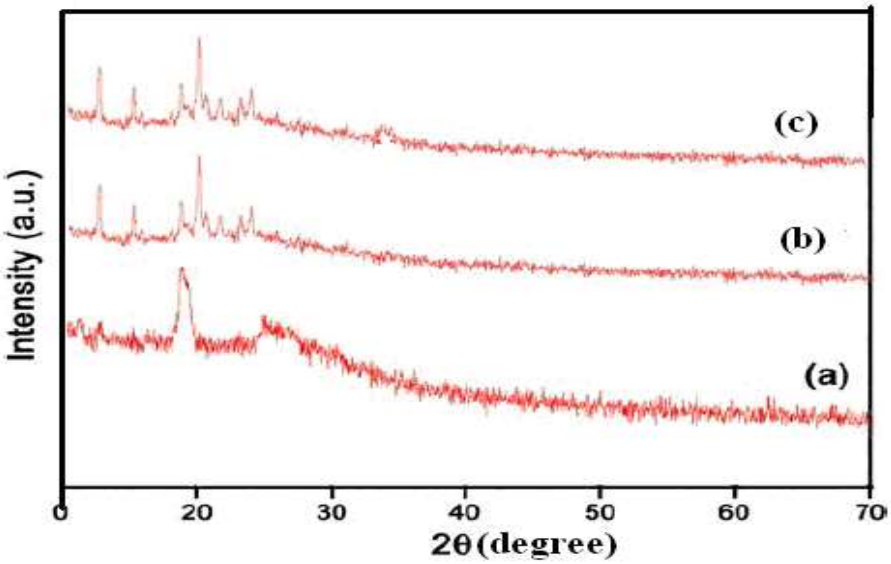


**(Figure4. X-ray diffraction data of a PMA/c-MWCNT (0%); b PMA/c-MWCNT (2%); c .PMA/c-MWCNT (5%))**

The X-ray diffraction data for PMA and PMA/c-MWCNT composites of 2 and 5% are shown in Figure**.**4. The spectrum of bare copolymer depicts two peaks at the region of 2θ=18.1 °C and 25.2 °C shown in Figure.4a which arise from the momentum transfer perpendicular to the chain direction. XRD pattern of nanocomposite (Figure**.** 4b and 4c) shows that there are two obvious phases: the copolymer phase and the c-MWCNTs phase which has several sharp peaks at 2θ=6.2 °C, 11.8 °C, 19.4 °C, 20.9 °C, 23.8 °C, and 26.3 °C. It implies that the nanocomposites possess a more crystalline nature than the bare copolymer. This can be attributed to the fact that the crystalline phase of the copolymer is most probably developed in the nanocomposite matrix. The appearance of a small peak at 2θ value of 26.3 °C suggests the existence of c-MWCNTs in the nanocomposite.

**TGA and DSC**

TGA and DSC curves of bare polymer and PMA/c-MWCNTs nanocomposite with 5% c-MWCNT in nitrogen are shown in Figure.5 (a, b) and the results are compared with the bare copolymer. All the samples followed the similar decomposition trend with exhibition of a gradual weight loss. The prepared copolymer exhibits a three-step weight loss. The first weight-loss step in the TGA curve of the copolymer between 50 °C and 140 °C corresponds to the loss of moisture, volatilization of the solvent, and adsorbed HCl. The second step between 170 °C and 260 °C is due to the loss of dopant and the concurrent evolution of $CO_2$. The third step occurring between 420 °C and 600 °C corresponds to the final degradation of

the copolymer. However, it was found that the thermal stability of nanocomposite is higher than the bare copolymer which is obviously related to the existence of thermally stable c-MWCNTs.

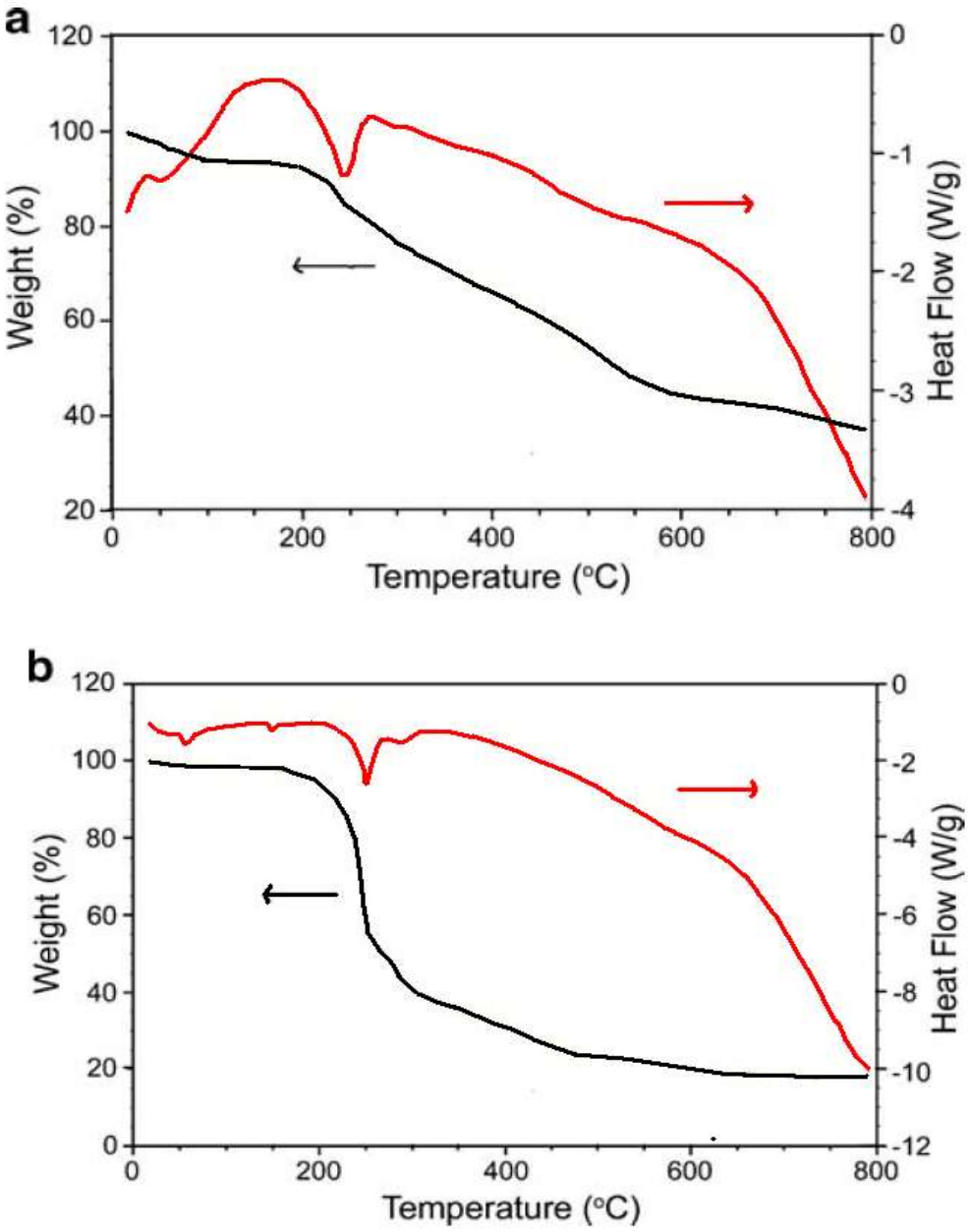


**(Figure 5. TGA and DSC curves of a bare copolymer and b nanocomposite with 5% c-MWCNTs in nitrogen)**

DSC curves of the bare copolymer and nanocomposite exhibit two-step degradation. The first endothermic peak in the DSC curve correlates to the loss of adsorbed HCl and moisture in the TG study. The second endothermic peak between 230 °C and 270 °C can be attributed to the morphological changes and disruption of inter- and intermolecular hydrogen bonding. From

DSC measurements, it is clear that the incorporation of MWCNTs into the copolymer resulted in an increase in the crystalline temperature (heating scan) relative to the bare copolymer. This behavior is expected and associated with the strong heterogeneous nucleation effect of the MWCNTs in the nanocomposite system. As the loading ratio of MWCNTs increases, the crystalline temperature of nanocomposite material increases.

**CONDUCTIVITY**

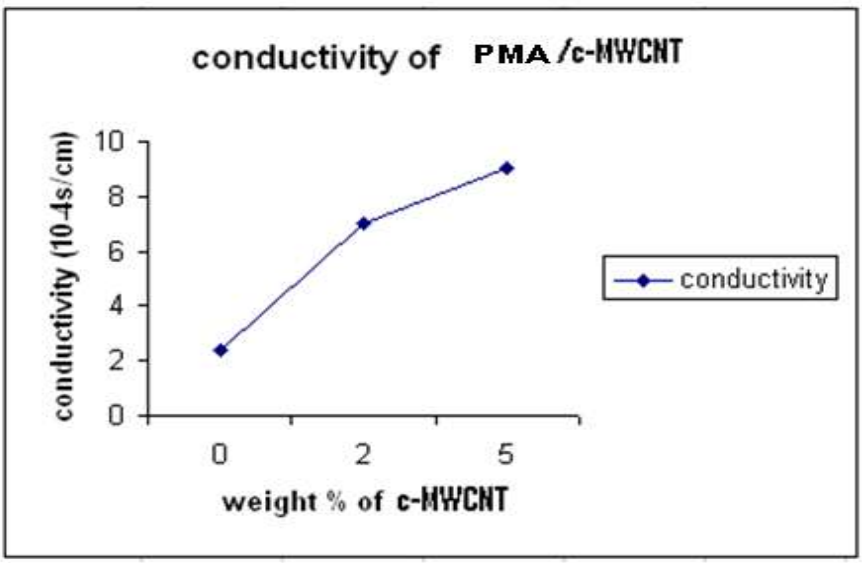


**(Figure.6. Conductivity versus the weight percent of c -MWCNT/PMTcomposites).**

The electrical conductivities PMA and PMA/c- MWCNT composites are measured using the standard Van Der Pauw DC four-probe method and shown in Figure6. The conductivity of MWCNT is about 0.2 S/cm. The conductivities of PMA synthesized in the presence of hydrochloric acid shows a room temperature conductivity of $2.4\times10^{-4}$ S/cm . The lower room temperature conductivity of PMA than PANI probably has something to do with its substituted group and low protonic acid doping degree. Meanwhile, the addition of 2 wt.% c-MWCNT into PMA, the conductivity at room temperature increases from 2.4 to $7\times10^{-4}$ S/cm. With the continuous increase in the content of c-MWCNT, the conductivity at room temperature gradually increases from $7\times10^{-4}$ S/cm for 2 wt.% MWCNT-containing PMA/c-MWCNT composites to $9\times10^{-4}$S/cm for 5 wt.% MWCNTcontaining PMA/c-MWCNT composites. The conductivities of PMA/c-MWCNT composites with 5 wt.% c-MWCNTs content at room temperature are much more higher than those of PMA without c-MWCNTs. The reason is probably that c-MWCNTs serve as a "conducting bridge" between the PMT conducting domains, which increases the effective percolation.

## 4. CONCLUSION

PMA/c-MWCNTs nanocomposites were successfully synthesized via in situ polymerization method. SEM and TEM measurement ascertained that the c-MWCNTs were homogeneously dispersed in the copolymer matrix. The interaction between c-MWCNTs and copolymer chain was confirmed by FTIR. The nanocomposites showed higher thermal stabilities in comparison with the bare copolymer was confirmed by TGA and DSC. Room temperature conductivity of nanocomposite increased several times as increasing of percentage of c-MWCNT .The highly ordered structures of nanocomposites were confirmed by XRD patterns. In addition, the versatility of this method could be extended to prepare other polymer/ CNT nanocomposites by choosing appropriate experimental conditions.

## REFERENCE

1. Mintmire J. W, Dunlap B. I, White C. T, Phys Rev Lett, 1992; 68: 631.
2. Overney G, Zhong W, Tomanek D. Z. Phys D, 1993; 27: 93.
3. Iijima S, Ichihashi T, Nature, 1993; 363: 603.
4. Wong E W, Sheehan P. E, Liebe C. M, Science, 1997; 277; 1975.
5. Schadler L. S, Giannaris S. C, Ajayan P. M, Phys Lett, 1998; 73: 3842.
6. Frank S, Poncharal P, Wang Z. L, Heer W. A, Science, 1998; 290: 1744.
7. Jans S. J, Verschueren A. R. M, Dekker C. Nature, 1998; 393: 49.
8. Dai H, Hafner J. H, Rinzler A. G, Colbert D. T, Smalley R. E. Nature, 1996; 384: 147.
9. Tang B. Z, Xu H. Y. Macromolecules, 1999; 32: 2569.
10. Curran S. A, Ajayan P. M, Blau W. J, Carroll D. L, Coleman J. N, Dalton A. B, Davey A. P, Drury A, McCarthy B, Maier S, Stevens A, Adv Mater, 1998; 10: 1091.
11. Ago H, Petritsch H. K, Shaffer M. S. P, Windle A. H, Friend R. H. Adv Mater, 1999; 11: 1281.
12. Musa I, Baxendale M, Amaratunga G. A. J, Eccleston W. Synth Met, 1999; 102: 1250.
13. Sun X. H, Li C. P, Wong N. B, Lee C. S, Lee S. T, Teo B. K. J Am Chem Soc, 2002; 124: 14464.
14. Skotheim T. A, Elsenbaumer R. L, Reynolds, J. R. Handbook of Conducting Polymers; Marcel Dekker: New York, 1997.
15. Premamoy G, Samir K. S, Amit C. Eur Polym J, 1999; 35: 699.
16. Hassanien A, Gao M, Tokumoto M, Dai L. Chem Phys Lett, 2001; 342: 479.
17. Deng J, Ding X, Zhang W, Peng Y, Wang J, Long X, Albert L. P, Chan A. S. C, Eur Polym J, 2002; 38: 2497.

18. Maser W. K, Benito A. M, Callejas M. A, Seeger T, Martinez M. T, Schreiber J, Muszynski J, Chauvet O, Osvath Z, Koos A. A, Biro L. P, Mater Sci Eng C, 2003; 23: 87.
19. Yupeng G, Kaifeng Y, Zichen W, Hongding X, Carbon, 2002; 41: 1645.
20. Feng W, Bai X. D, Lian Y. Q, Liang J, Wang X. G, Yoshono K. Carbon, 2003; 41: 1551.
21. Maiyalagan T, (2008), Journal of Power Sources, 179; 443.
22. Li X. G, Huang M. R, Chen R. F, Jin Y. and Yang Y. L, J. Appl. Polym. Sci, 2001; 81: 3107.
23. Cataldo F, J. Eur. Polym, 1996; 32: 43.
24. Li X. G, Huang M. R, and Duan W, Chem. Rev, 2002; 102**:** 2925
25. Prokeš J, Stejskal J, K˘rivka I. and Tobolková E, Synth. Met, 1999; 102: 1205.
26. Haldorai Y, Lyoo W. S, and Shim J. J, Colloid Polym Sci, 2009; 287: 1273.
27. Wu T. M, Lin Y. W, and Liao C. S, Carbon, 2005; 43**:** 734.
28. Sestrem R. H, Ferreira D. C, Landers R, Temperini M. L. A. and do Nascimento G. M. D, Polymer, 2009; 50**:** 6043.